Expanding the toolbox of coinage bond: Adducts involving new gold(III) derivatives and bioactive molecules

Andrea Pizzi,[a] Miriam Calabrese,[a] Andrea Daolio,[a] Maurizio Ursini,[a] Antonio Frontera,[b] and Giuseppe Resnati*[a]

ELECTRONIC SUPPLEMENTARY INFORMATION

a   NFMLab, Department of Chemistry, Materials, and Chemical Engineering "Giulio Natta"
     Politecnico di Milano
     via L. Mancinelli 7; I-20131 Milano, Italy
     E-Mail: giuseppe.resnati@polimi.it
b   Department of Chemistry
     Universitat de les Illes Balears
     Crta. de Valldemossa km 7.5, 07122 Palma de Mallorca (Baleares), Spain

Table Of Content:

S1. Materials and Methods.

S.1.1. Materials. Chloroauric acid (HAuCl$_4$·xH$_2$O), potassium tetrabromidoaurate (KAuCl$_4$) and pyridine derivatives were acquired from commercial suppliers (Sigma-Aldrich, TCI America) and used without further purification.

S.1.2. Characterization of the compounds.

FT-IR spectra were obtained using a Nicolet Nexus FT-IR spectrometer equipped with UATR unit.

*Synthesis of AuCl$_3$·cotinine (*1a*)*. A solution of chloroauric acid (0.02 mmol) in methanol (2 mL) was dropped in a clear borosilicate vial containing an equimolar amount of cotinine in the same solvent (3 mL). Yellow crystals of **1a** with an elongated block shape and suitable for single crystal X-Ray diffraction were obtained in 24 hours by slow evaporation of the solvent. FT-IR (selected bands, cm^{-1}) 3044, 1672, 1447, 1395, 1253, 1192, 1152, 1110, 918, 814, 689. Elemental Analysis for: C$_{10}$H$_{12}$N$_2$OAuCl$_3$, % calc. (found): C, 25.05 (25.10); H, 2.52 (2.53); Cl, 22.18 (22.12); N, 5.84 (5.84).

*Synthesis of AuCl$_3$·3-fluoropyridine (*1b*)*. Yellow crystals of **1b** with an elongated block shape and suitable for single crystal X-Ray diffraction were obtained by using a procedure similar to that used for **1a**. FT-IR (selected bands, cm^{-1}) 1551, 1471, 1442, 1347, 1307, 1281, 1241, 1177, 1101, 1035. Elemental Analysis for C$_5$H$_4$NFAuCl$_3$, % calc. (found): C, 15.00 (14.97); H, 1.01 (1.02); N, 3.50 (3.52).

*Synthesis of AuCl$_3$·3-chloro pyridine (*1c*)*. Yellow crystals of **1c** with an elongated block shape and suitable for single crystal X-Ray diffraction were obtained by using a procedure similar to that used for **1a**. FT-IR (selected bands, cm^{-1}) 1594, 1558, 1469, 1427, 1321, 1247, 1195, 1129, 1122, 1089, 1068, 1029. Elemental Analysis for C$_5$H$_4$NAuCl$_4$, % calc. (found): C, 14.41 (14.37); H, 0.97 (0.96); Cl, 34.02 (34.12); N, 3.36 (3.31).

*Synthesis of AuCl$_3$·3-bromo pyridine (*1d*)*. Yellow crystals of **1d** with an elongated block shape and suitable for single crystal X-Ray diffraction were obtained by using a procedure similar to that used for **1a**. FT-IR (selected bands, cm^{-1}) 1635, 1560, 1467, 1423, 1403, 1240, 1198, 1122, 1109, 1064. Elemental Analysis for C$_5$H$_4$NBrAuCl$_3$, % calc. (found): C, 13.02 (13.03); H, 0.87 (0.86); N, 3.04 (3.04).

Synthesis of AuCl₃·3-iodo pyridine ($\textbf{1e}$*)*. Yellow crystals of **1e** with an elongated block shape and suitable for single crystal X-Ray diffraction were obtained by using a procedure similar to that used for **1a**. FT-IR (selected bands, cm⁻¹) 1588, 1549, 1473, 1463, 1425, 1415, 1329, 1239, 1195, 1117, 1102, 1084, 1062, 1025. Elemental Analysis for $C_5H_4NIAuCl_3$, % calc. (found): C, 11.81 (11.82); H, 0.79 (0.78); N, 2.76 (2.76).

Synthesis of AuBr₃·cotinine ($\textbf{1f}$*)*. A solution of $KAuBr_4$ (0.02 mmol) in methanol (2 mL) was dropped in a clear borosilicate vial containing an equimolar amount of cotinine in the same solvent (3 mL). The solution was then heated at 50 °C for 12 hours. Orange crystals of **1f** with an elongated block shape and suitable for single crystal X-Ray diffraction were obtained in 24 hours by slow evaporation of the solvent. FT-IR (selected bands, cm⁻¹) 1675, 1447, 1394, 1308, 1252, 1192, 1153, 1109, 916, 816, 691. Elemental Analysis for: $C_{10}H_{12}N_2OAuBr_3$, % calc. (found): C, 19.06 (19.02); H, 1.97 (1.95); Br, 39.11 (39.16); N, 4.57 (4.58).

Synthesis of AuBr₃·3-fluoro pyridine ($\textbf{1g}$*)*. Orange crystals of **1g** with an elongated block shape and suitable for single crystal X-Ray diffraction were obtained by using a procedure similar to that used for **1f**. FT-IR (selected bands, cm⁻¹) 1610, 1579, 1479, 1441, 1417, 1260, 1249, 1186, 1117, 1098, 1049, 1026. Elemental Analysis for $C_5H_4NFAuBr_3$, % calc. (found): C, 11.25 (11.24); H, 0.76 (0.78); N, 2.62 (2.61).

S2. Crystallographic Details.

S.2.1. General Remarks. The single crystal data of the compounds were collected at room temperature using a Bruker SMART APEX II CCD area detector diffractometer. Data collection, unit cell refinement and data reduction were performed using Bruker SAINT. Structures were solved by direct methods using SHELXT[1] and refined by full-matrix least-squares on F^2 with anisotropic displacement parameters for the non-H atoms using SHELXL-2016/6[2]. Absorption correction was performed based on multi-scan procedure using SADABS. Structure analysis was aided by use of the programs PLATON[3]. The hydrogen atoms were calculated in ideal positions with isotropic displacement parameters set to $1.2 \times U_{eq}$ of the attached atom. In compound **1a**, the reported low fraction of measured data is due to the bad quality of the needle-shaped crystal selected for the data collection. Many crystals of the same sample have been tested, and the best one was selected. In compound **1b**, high residual peaks of electron density have been found around the gold atom. As in all the samples of this work, empirical methods for absorption correction have been applied, trying to find the best compromise between data quality and data completeness. In order to minimize/avoid these residual peaks around the metal, analytical methods for absorption correction would be needed, although the quality of these crystals, makes it unfeasible. We tested many crystals of **1b** and we collected the best one.

S.2.2. Crystallographic details and Figures for compounds 1a-1g.

Table S.1 Crystal data and structure refinement for **1a**.

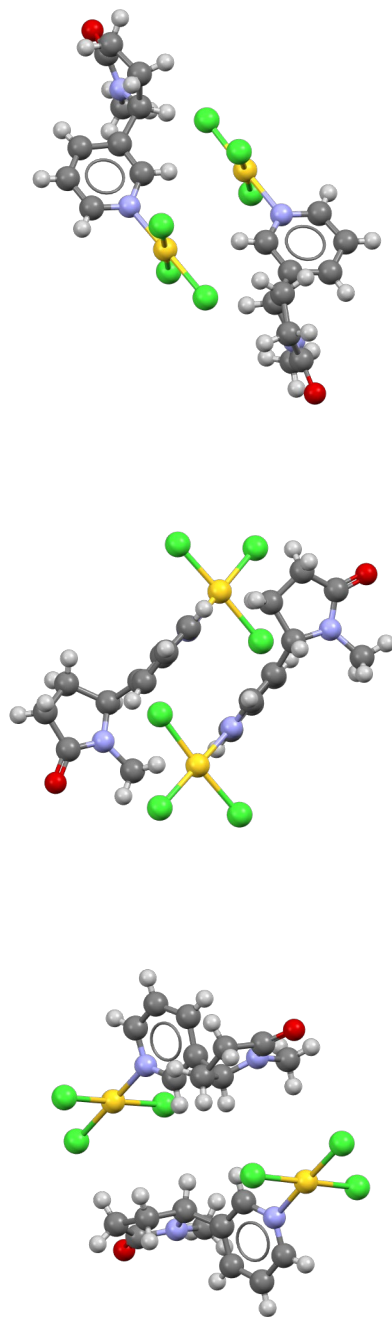| Identification code	**1a**
Empirical formula	$C_{10}H_{12}AuCl_3N_2O$
Formula weight	479.53
Temperature/K	296(2)
Crystal system	triclinic
Space group	P1
a/Å	7.4947(17)
b/Å	9.945(3)
c/Å	10.000(2)
α/°	85.660(13)
β/°	69.881(12)
γ/°	78.186(12)
Volume/Å^3	685.0(3)
Z	2
$\rho_{calc}g/cm^3$	2.325
μ/mm^{-1}	11.307
F(000)	448.0
Crystal size/mm^3	0.08 × 0.06 × 0.04
Radiation	MoKα (λ = 0.71073)
2Θ range for data collection/°	6.046 to 66.954
Index ranges	-11 ≤ h ≤ 10, -14 ≤ k ≤ 14, -13 ≤ l ≤ 15
Reflections collected	12301
Independent reflections	7361 [R_{int} = 0.0434, R_{sigma} = 0.0910]
Data/restraints/parameters	7361/3/300
Goodness-of-fit on F^2	0.867
Final R indexes [I>=2σ (I)]	R_1 = 0.0331, wR_2 = 0.0578
Final R indexes [all data]	R_1 = 0.0668, wR_2 = 0.0665
Largest diff. Peak/hole / e Å^{-3}	1.46/-1.67
Flack parameter	0.06(2)
CCDC Number	2144993

Figure S.1. Unit cell content of **1a** along the three crystal axes; top *a*, middle *b*, bottom *c*. Color code *grey* carbon, *whitish* hydrogen, *light blue* nitrogen, *red* oxygen, *green* chloride, *yellow* gold.

Table S.2 Crystal data and structure refinement for **1b**.

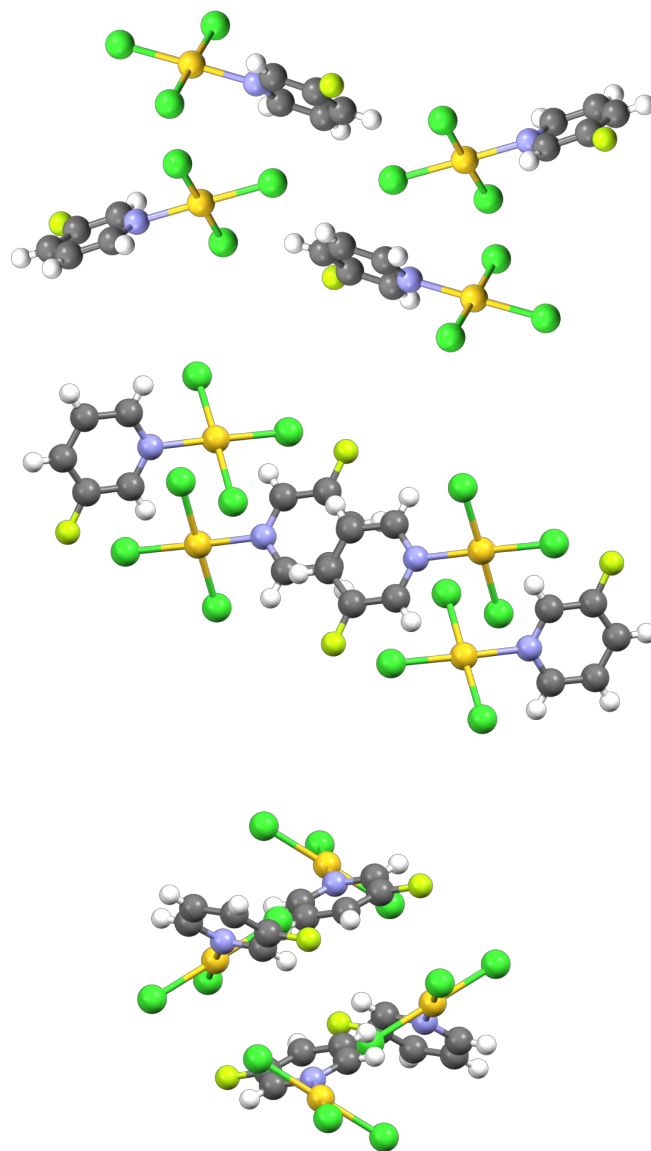| Identification code	**1b**
Empirical formula	$C_5H_4NFCl_3AuO$
Formula weight	400.41
Temperature/K	296(2)
Crystal system	monoclinic
Space group	$P2_1/n$
a/Å	6.6793(11)
b/Å	8.2420(13)
c/Å	16.356(3)
α/°	90
β/°	94.540(8)
γ/°	90
Volume/Å^3	897.6(3)
Z	4
$\rho_{calc}g/cm^3$	2.963
μ/mm^{-1}	17.230
F(000)	720.0
Crystal size/mm^3	0.2 × 0.08 × 0.08
Radiation	MoKα (λ = 0.71073)
2Θ range for data collection/°	6.424 to 86.18
Index ranges	-10 ≤ h ≤ 12, -15 ≤ k ≤ 14, -31 ≤ l ≤ 30
Reflections collected	23205
Independent reflections	6546 [R_{int} = 0.0781, R_{sigma} = 0.0791]
Data/restraints/parameters	6546/0/101
Goodness-of-fit on F^2	1.047
Final R indexes [I>=2σ (I)]	R_1 = 0.0637, wR_2 = 0.1581
Final R indexes [all data]	R_1 = 0.1078, wR_2 = 0.1795
Largest diff. peak/hole / e Å^{-3}	6.88/-5.91
CCDC Number	2144969

Figure S.2. Unit cell content of **1b** along the three crystal axes; top *a*, middle *b*, bottom *c*. Color code *gray* carbon, *whitish* hydrogen, *light blue* nitrogen, *lime* fluorine, *green* chlorine, *yellow* gold.

Table S.3 Crystal data and structure refinement for **1c**.

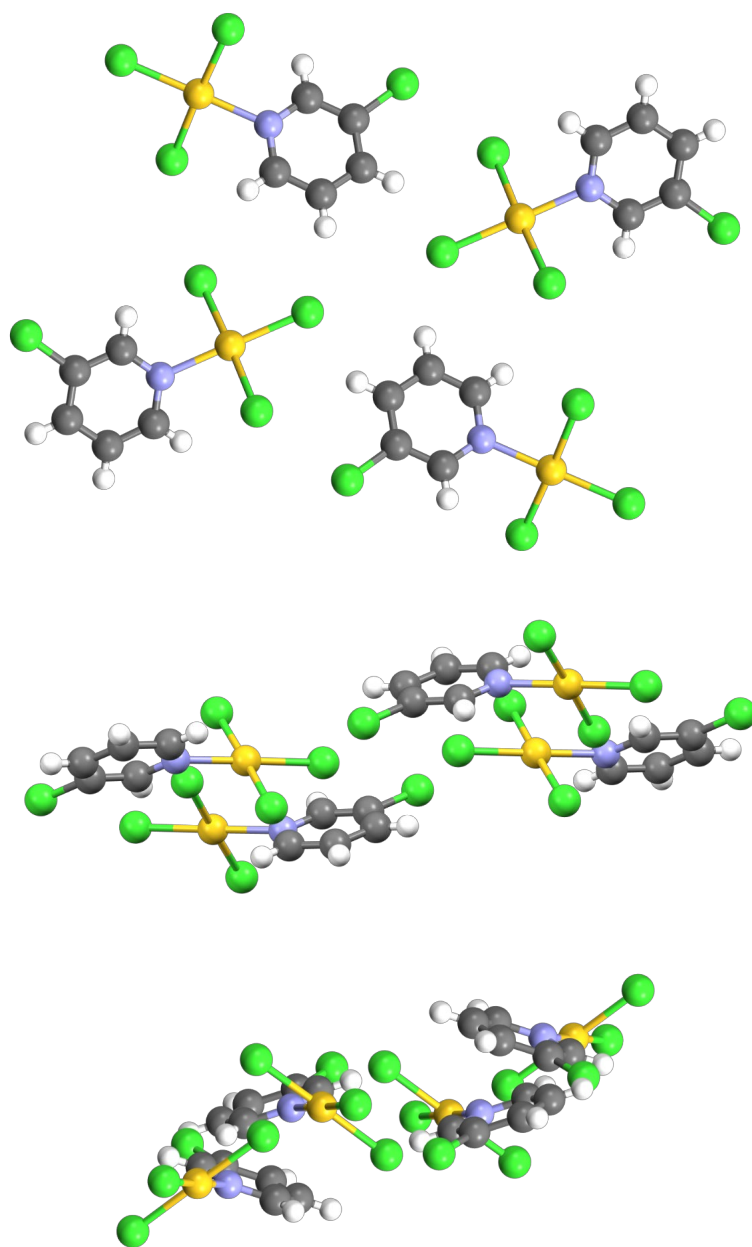| Identification code	**1c**
Empirical formula	$C_5H_4NCl_4Au$
Formula weight	416.86
Temperature/K	296(2)
Crystal system	monoclinic
Space group	$P2_1/n$
a/Å	4.0879(5)
b/Å	13.4780(19)
c/Å	17.229(2)
α/°	90
β/°	90.976(5)
γ/°	90
Volume/Å^3	949.1(2)
Z	4
ρ_{calc}g/cm^3	2.917
μ/mm^{-1}	16.559
F(000)	752.0
Crystal size/mm^3	0.2 × 0.08 × 0.08
Radiation	MoKα (λ = 0.71073)
2Θ range for data collection/°	7.678 to 61.846
Index ranges	-5 ≤ h ≤ 5, -18 ≤ k ≤ 19, -24 ≤ l ≤ 24
Reflections collected	18882
Independent reflections	2947 [R_{int} = 0.0333, R_{sigma} = 0.0241]
Data/restraints/parameters	2947/0/100
Goodness-of-fit on F^2	1.062
Final R indexes [I>=2σ (I)]	R_1 = 0.0200, wR_2 = 0.0359
Final R indexes [all data]	R_1 = 0.0325, wR_2 = 0.0390
Largest diff. peak/hole / e Å^{-3}	0.81/-0.89
CCDC Number	2144976

Figure S.3 Unit cell content of **1c** along the three crystal axes; top *a*, middle *b*, bottom *c*. Color code *grey* carbon, *whitish* hydrogen, *light blue* nitrogen, *green* chlorine, *yellow* gold.

Table S.4 Crystal data and structure refinement for **1d**.

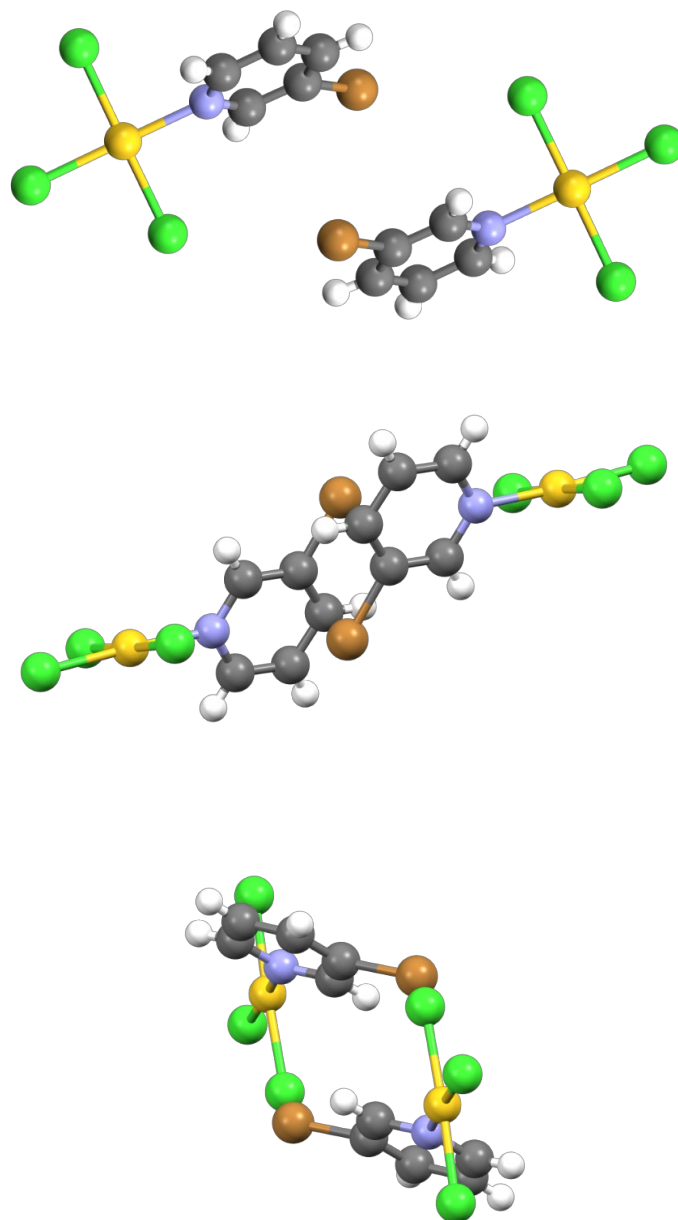| Identification code	**1d**
Empirical formula	$C_5H_4NCl_3BrAu$
Formula weight	461.32
Temperature/K	296(2)
Crystal system	triclinic
Space group	P-1
a/Å	7.0468(9)
b/Å	7.9600(10)
c/Å	9.2442(12)
α/°	80.193(9)
β/°	78.165(8)
γ/°	80.695(8)
Volume/Å^3	495.75(11)
Z	2
ρ_{calc}g/cm^3	3.090
μ/mm^{-1}	19.612
F(000)	412.0
Crystal size/mm^3	0.2 × 0.08 × 0.08
Radiation	MoKα (λ = 0.71073)
2Θ range for data collection/°	7.402 to 60.27
Index ranges	-9 ≤ h ≤ 9, -11 ≤ k ≤ 11, -13 ≤ l ≤ 13
Reflections collected	9765
Independent reflections	2803 [R_{int} = 0.0561, R_{sigma} = 0.0689]
Data/restraints/parameters	2803/0/100
Goodness-of-fit on F^2	0.960
Final R indexes [I>=2σ (I)]	R_1 = 0.0392, wR_2 = 0.0647
Final R indexes [all data]	R_1 = 0.0802, wR_2 = 0.0747
Largest diff. peak/hole / e Å^{-3}	0.95/-1.01
CCDC Number	2144963

Figure S.4 Unit cell content of **1d** along the three crystal axes; top *a*, middle *b*, bottom *c*. Color code *gray* carbon, *whitish* hydrogen, *light blue* nitrogen, *green* chlorine, *brown* bromine, *yellow* gold.

Table S.5 Crystal data and structure refinement for **1e**.

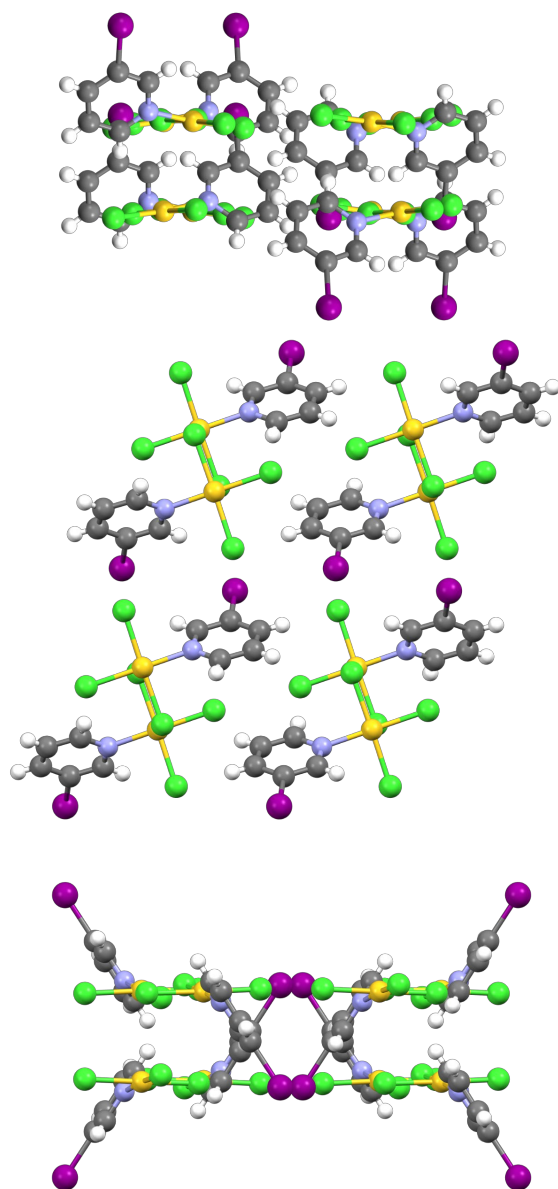| Identification code	**1e**
Empirical formula	$C_5H_4NCl_3IAu$
Formula weight	508.31
Temperature/K	296(2)
Crystal system	monoclinic
Space group	C2/c
a/Å	18.5724(12)
b/Å	6.8315(4)
c/Å	16.2536(10)
α/°	90
β/°	103.388(2)
γ/°	90
Volume/Å^3	2006.2(2)
Z	8
$\rho_{calc}g/cm^3$	3.366
μ/mm^{-1}	18.480
F(000)	1792.0
Crystal size/mm^3	0.009 × 0.006 × 0.003
Radiation	MoKα (λ = 0.71073)
2Θ range for data collection/°	6.376 to 73.676
Index ranges	-29 ≤ h ≤ 27, -10 ≤ k ≤ 11, -26 ≤ l ≤ 24
Reflections collected	22700
Independent reflections	4292 [R_{int} = 0.0347, R_{sigma} = 0.0276]
Data/restraints/parameters	4292/0/100
Goodness-of-fit on F^2	1.025
Final R indexes [I>=2σ (I)]	R_1 = 0.0250, wR_2 = 0.0444
Final R indexes [all data]	R_1 = 0.0443, wR_2 = 0.0513
Largest diff. peak/hole / e Å^{-3}	2.05/-1.33
CCDC Number	2144977

Figure S.5 Unit cell content of **1e** along the three crystal axes; top *a*, middle *b*, bottom *c*. Color code *grey* carbon, *whitish* hydrogen, *light blue* nitrogen, *green* chlorine, *purple* iodine, *yellow* gold.

Table S.6 Crystal data and structure refinement for **1f**.

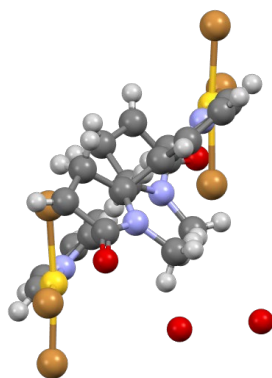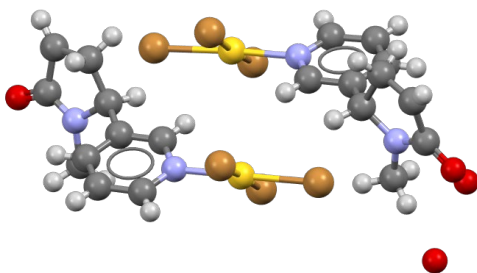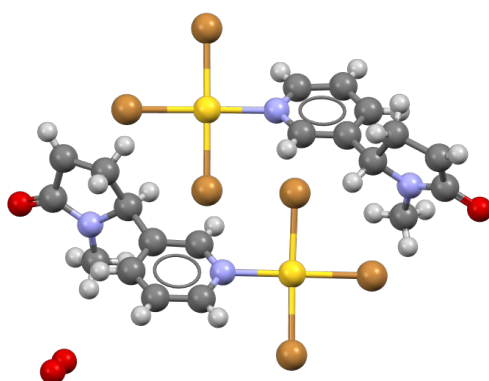| Identification code	**1f**
Empirical formula	$C_{10}H_{11}AuBr_3N_2O_2$
Formula weight	627.90
Temperature/K	296(2)
Crystal system	triclinic
Space group	P1
a/Å	7.3049(4)
b/Å	7.9398(4)
c/Å	14.1403(8)
α/°	91.892(2)
β/°	101.920(3)
γ/°	99.075(2)
Volume/Å^3	790.57(7)
Z	2
ρ_{calc}g/cm^3	2.638
μ/mm^{-1}	16.880
F(000)	570.0
Crystal size/mm^3	0.08 × 0.04 × 0.02
Radiation	MoKα (λ = 0.71073)
2Θ range for data collection/°	5.782 to 67.542
Index ranges	-10 ≤ h ≤ 11, -12 ≤ k ≤ 11, -18 ≤ l ≤ 20
Reflections collected	17402
Independent reflections	8282 [R_{int} = 0.0252, R_{sigma} = 0.0456]
Data/restraints/parameters	8282/3/318
Goodness-of-fit on F^2	0.958
Final R indexes [I>=2σ (I)]	R_1 = 0.0250, wR_2 = 0.0430
Final R indexes [all data]	R_1 = 0.0391, wR_2 = 0.0455
Largest diff. peak/hole / e Å^{-3}	0.97/-0.82
Flack parameter	0.043(10)
CCDC Number	214491

Figure S.6 Unit cell content of **1f** along the three crystal axes; top *a*, middle *b*, bottom *c*. Color code *grey* carbon, *whitish* hydrogen, *light blue* nitrogen, *red* oxygen, *brown* bromine, *yellow* gold.

Table S.7 Crystal data and structure refinement for **1g**.

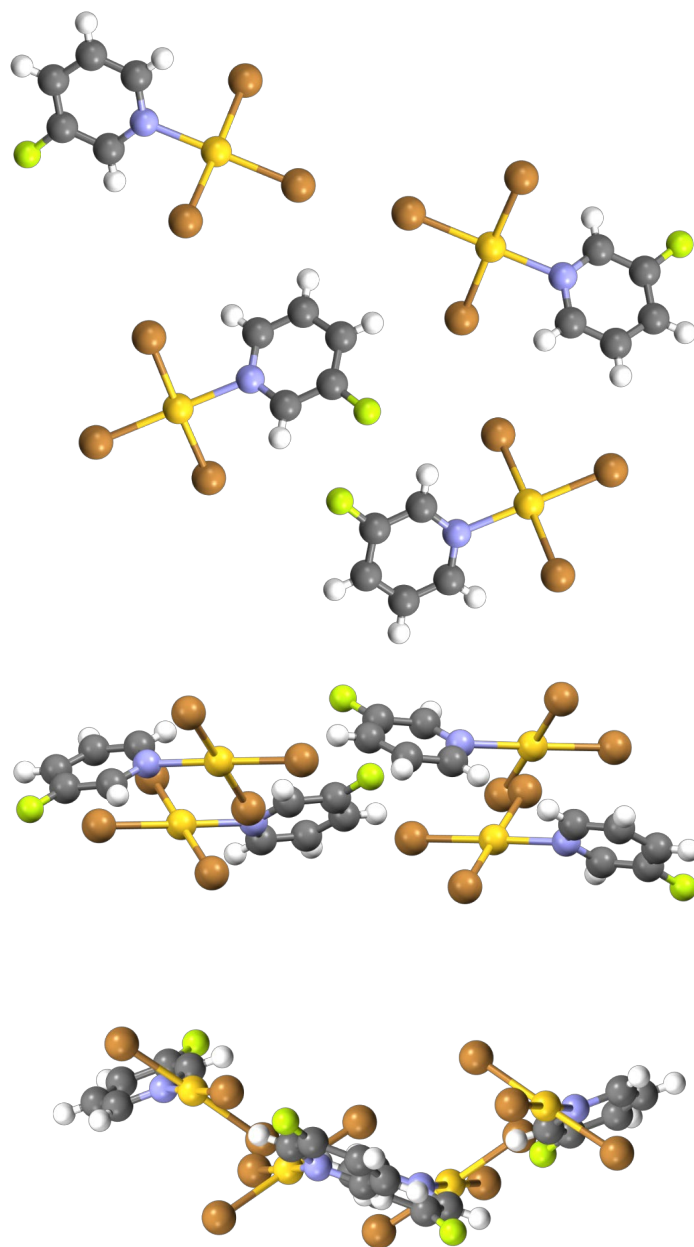| Identification code	**1g**
Empirical formula	$C_5H_4AuBr_3FN$
Formula weight	533.79
Temperature/K	296(2)
Crystal system	orthorhombic
Space group	$P2_12_12_1$
a/Å	4.1948(4)
b/Å	13.8237(14)
c/Å	16.8348(18)
α/°	90
β/°	90
γ/°	90
Volume/Å^3	976.21(17)
Z	4
ρ_{calc}g/cm^3	3.632
μ/mm^{-1}	27.302
F(000)	936.0
Crystal size/mm^3	0.009 × 0.006 × 0.003
Radiation	MoKα (λ = 0.71073)
2Θ range for data collection/°	7.628 to 46.362
Index ranges	-4 ≤ h ≤ 4, -15 ≤ k ≤ 15, -18 ≤ l ≤ 18
Reflections collected	6125
Independent reflections	1390 [R_{int} = 0.0884, R_{sigma} = 0.0625]
Data/restraints/parameters	1390/0/101
Goodness-of-fit on F^2	1.000
Final R indexes [I>=2σ (I)]	R_1 = 0.0333, wR_2 = 0.0697
Final R indexes [all data]	R_1 = 0.0393, wR_2 = 0.0719
Largest diff. peak/hole / e Å^{-3}	1.41/-1.17
Flack parameter	0.48(4)
CCDC Number	2144992

Figure S.7 Unit cell content of **1g** along the three crystal axes; top *a*, middle *b*, bottom *c*. Color code *grey* carbon, *whitish* hydrogen, *light blue* nitrogen, *lime* fluorine, *brown* bromine, *yellow* gold.

S3. CSD Surveys.

Table S.8 Number of hits on the CSD displaying tetravalent gold compounds bound to three halogens and a pyridyl substituent. In red, hits displaying a contact between the gold atom and a nucleophile (N, P, O, S, Se, F, Cl, Br, I considered) shorter than the sum of the respective van der Waals radii of involved atoms and establishing X/N-Au⋯Nu angles spanning the range 80 and 100°. In blue, hits displaying two of such contacts on the same gold atom. For this analysis, according to Batsanov's suggestion[4], the crystallographic vdW radius of gold was set to 210 pm.

DUCYEI	EHEXIA	KILFIV	OJELIA	VANPUY	WOQMUK
DUCYIM	EHEXOG	KUFNAB	PYAUCL10	VOYNUU	XAPXIY
BIRCUA	ELUVAK	LUVRIF	QIHVOS	VOYPAC	XIMWOI
BUVVAQ	FEYKIG	MIYYOL	SASREM	VOYPEG	YIDMAA
BUVVIY	HAFFEA	MIYZAY	SASREM01	WIRFUA	ZUHNIB
BUWTIY	HAFFIE	MIYZEC	SASRIQ	WIRGAH	ZUHNOH
BUWVUM	HIHCIK	MOCFER	TIRMEP	WOQLET	ZUHNUN
DOYPOY	HOSHII	MOCFUH	UQIBEC	WOQLIX	WUJKUK
DOYPOY01	HOSHUU	NIYTIA	UZIMEW	WOQMEU	

S4. Computational Details.

S.4.1. Theoretical methods. The energetic features of the adducts analyzed in this work were calculated at the PBE0[5]-D3[6]/def2-TZVP[7] level of theory using the crystallographic coordinates for the X-ray adducts. For gold, the inner shell electrons are modelled by ECPs (ECP-60 scheme),[8] which also accounts for scalar relativistic effects. The GAUSSIAN-16 program has been used for the energetic calculations[9] and NBO7 program for NBO analysis.[10] The basis set superposition error for the calculation of interaction energies has been corrected using the counterpoise method.[11] Molecular electrostatic potential (MEP) surfaces have been computed at the same level of theory and represented using several isovalues of electron density to map the electrostatic potential. The QTAIM[12] and NCIPlot[13,14] analyses has been performed using the AIMAll program[15] at the same level of theory.

S.4.2. QTAIM/NCIPLot analysis of compounds 1b-e and 1g

Figure S.8. shows the QTAIM/NCIplot analyses and dimerization energies of selected CiB assemblies of compounds **1b-e** and **1g**. The interaction energies range from –9.1 to –18.8 kcal/mol, depending on the number of CiBs, HBs and the electron donors. The interaction energies in the antiparallel dimers where X = Cl (**1d** and **1e**) are larger than those of parallel X = Br (**1g** and **1c**). The binding energy of the dimer **1b**, where only one CiB is formed, is approximately half of that of 1d and 1e (two CiBs I antiparallel orientation).

In all cases the CiB interactions are characterized by the corresponding bond CPs, bond paths and blue isosurfaces connecting the Au to the X-atoms. In case of the parallel orientation, additional π-stacking interactions are formed.
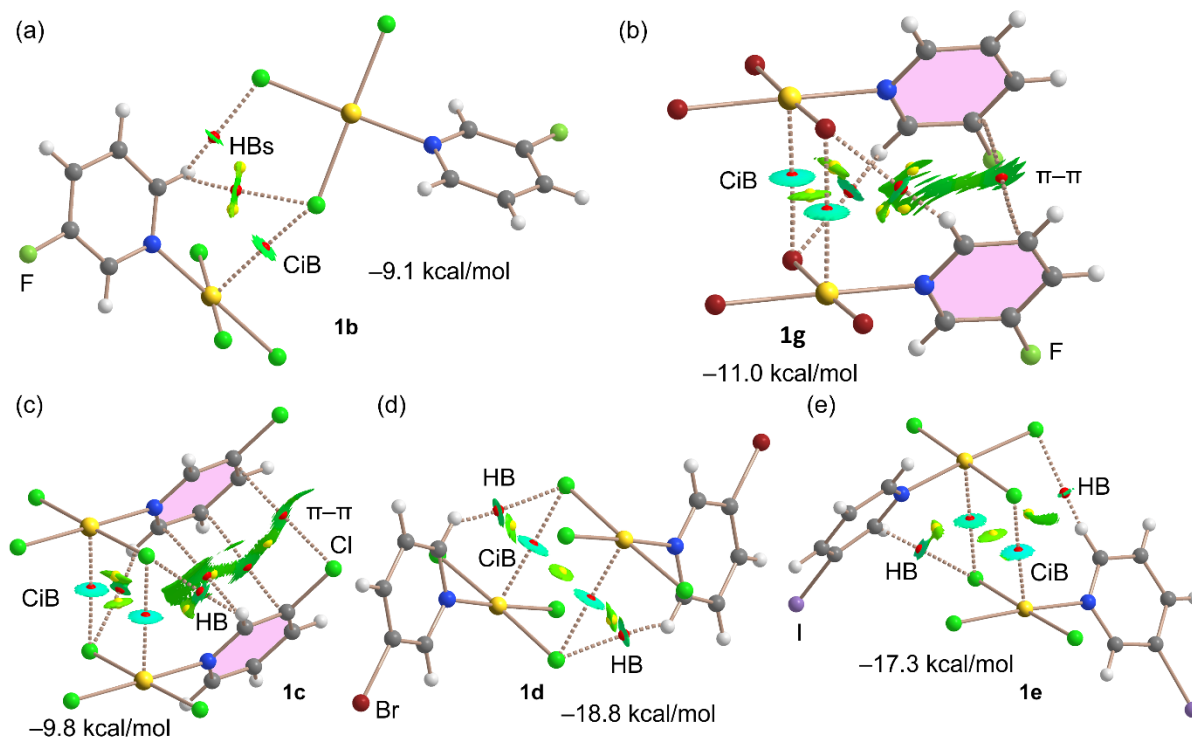
Figure S.8. QTAIM distribution of the critical points of the intermolecular bond and ring (red and yellow spheres, respectively) and bond paths for the dimeric assemblies of compounds **1b** (a), **1g** (b), **1c** (c), **1d** (d) and **1e** (e). The superimposed NCIplot isosurface (RDG isovalue=0.4 a.u.) is shown. The cut-off ρ=0.04 a.u. has been used. Color range: −0.025 a.u. ≤ (signλ_2)ρ ≤ 0.025 a.u. Level of theory: PBE0-D3/def2-TZVP.

S5. References.

(1)   Sheldrick, G. M. SHELXT – Integrated Space-Group and Crystal-Structure Determination. *Acta Crystallogr. Sect. A Found. Adv.* **2015**, *71* (1), 3–8, https://doi.org/10.1107/S2053273314026370.

(2)   Sheldrick, G. M. Crystal Structure Refinement with SHELXL. *Acta Crystallogr. Sect. C Struct. Chem.* **2015**, *71* (1), 3–8. https://doi.org/10.1107/S2053229614024218.

(3)   Spek, A. L. Structure Validation in Chemical Crystallography. *Acta Crystallogr. Sect. D Biol. Crystallogr.* **2009**, *65* (2), 148–155. https://doi.org/10.1107/S090744490804362X.

(4)   Batsanov, S. S. Van Der Waals Radii of Elements. *Inorg. Mater.* **2001**, *37* (9), 871–885. https://doi.org/10.1023/A:1011625728803.

(5)   Adamo, C.; Barone, V. Toward Reliable Density Functional Methods without Adjustable Parameters: The PBE0 Model. *J. Chem. Phys.* **1999**, *110* (13), 6158–6170. https://doi.org/10.1063/1.478522.

(6)   Grimme, S.; Antony, J.; Ehrlich, S.; Krieg, H. A Consistent and Accurate Ab Initio Parametrization of Density Functional Dispersion Correction (DFT-D) for the 94 Elements H-Pu. *J. Chem. Phys.* **2010**, *132* (15). https://doi.org/10.1063/1.3382344.

(7)   Weigend, F. Accurate Coulomb-Fitting Basis Sets for H to Rn. *Phys. Chem. Chem. Phys.* **2006**, *8* (9), 1057–1065. https://doi.org/10.1039/b515623h.

(8)   D. Andrae, U. Haeussermann, M. Dolg, H. Stoll and H. Preuss, *Theor. Chim. Acta* **1990**, *77*, 123−141, https://doi.org/10.1007/BF01114537.

(9)   M. J. Frisch, G. W. Trucks, H. B. Schlegel, G. E. Scuseria, M. A. Robb, J. R. Cheeseman, G. Scalmani, V. Barone, G. A. Petersson, H. Nakatsuji, X. Li, M. Caricato, A. V. Marenich, J. Bloino, B. G. Janesko, R. Gomperts, B. Mennucci, H. P. Hratchian, J. V. Ortiz, A. F. Izmaylov, J. L. Sonnenberg, Williams, F. Ding, F. Lipparini, F. Egidi, J. Goings, B. Peng, A. Petrone, T. Henderson, D. Ranasinghe, V. G. Zakrzewski, J. Gao, N. Rega, G. Zheng, W. Liang, M. Hada, M. Ehara, K. Toyota, R. Fukuda, J. Hasegawa, M. Ishida, T. Nakajima, Y. Honda, O. Kitao, H. Nakai, T. Vreven, K. Throssell, J. A. Montgomery Jr., J. E. Peralta, F. Ogliaro, M. J. Bearpark, J. J. Heyd, E. N. Brothers, K. N. Kudin, V. N. Staroverov, T. A. Keith, R. Kobayashi, J. Normand, K. Raghavachari, A. P. Rendell, J. C. Burant, S. S. Iyengar, J. Tomasi, M. Cossi, J. M. Millam, M. Klene, C. Adamo, R. Cammi, J. W. Ochterski, R. L. Martin, K. Morokuma, O. Farkas, J. B. Foresman, D. J. Fox, Wallingford, CT, **2016.**

(10)   E. D. Glendening, C. R. Landis, F. Weinhold, J. Comput. Chem. 2019, 40, 2234-2241, https://doi.org/10.1002/jcc.25873

(11)   Boys, S. F.; Bernardi, F. The Calculation of Small Molecular Interactions by the Differences of Separate Total Energies. Some Procedures with Reduced Errors. *Mol. Phys.* **1970**, *19* (4), 553–566. https://doi.org/10.1080/00268977000101561.

(12)   Bader, R. F. W. A Quantum Theory of Molecular Structure and Its Applications. *Chem. Rev.* **1991**, *91* (5), 893–928. https://doi.org/10.1021/cr00005a013.

(13)   E. R. Johnson, S. Keinan, P. Mori-Sánchez, J. Contreras-García, A. J. Cohen, W. Yang, *J. Am. Chem. Soc.* **2010**, *132*, 6498-6506, https://doi.org/10.1021/ja100936w.

(14)   J. Contreras-García, E. R. Johnson, S. Keinan, R. Chaudret, J.-P. Piquemal, D. N. Beratan, W. Yang, *J. Chem. Theory Comput.* **2011**, *7*, 625-632., https://doi.org/10.1021/ct100641a

(15)   T. A. Keith, TK Gristmill Software, OverlandPark KS, USA **2019**.